

# Large Within-Die Gate Delay Variations in Sub-Threshold Logic Circuits at Low Temperature

Ryo Takahashi, *Student Member, IEEE*, Hidehiro Takata, Tadashi Yasufuku, *Member, IEEE*, Hiroshi Fuketa, *Member, IEEE*, Makoto Takamiya, *Member, IEEE*, Masahiro Nomura, *Member, IEEE*, Hirofumi Shinohara, and Takayasu Sakurai, *Fellow, IEEE*

**Abstract**—Temperature dependence of 256 within-die random gate delay variations in sub-threshold logic circuits is measured in 40-nm CMOS test chips. When the temperature is reduced from 25°C to –40°C, the sigma/average ( $\sigma/\mu$ ) of the gate delay at 0.3 V increases by 1.4 times. A newly developed model shows that  $\sigma/\mu$  of the gate delay is proportional to  $1/T$  for the first time, where  $T$  is the absolute temperature.

**Index Terms**—Delay variations, device matrix array (DMA), sub-threshold, temperature.

## I. INTRODUCTION

**S**UB-THRESHOLD circuits, which operate at a lower supply voltage ( $V_{DD}$ ) than threshold voltage ( $V_{TH}$ ), are one of promising solutions to achieve ultra-low power operation [1]. When  $V_{DD}$  is reduced from the above-threshold region to the sub-threshold region, the gate delay variations (= sigma/average(=  $\sigma/\mu$ )) due to the within-die random  $V_{TH}$  variation sharply increase [2], because the sub-threshold current has an exponential dependence on  $V_{TH}$ . In the sub-threshold logic circuits, the average ( $\mu$ ) and the variation ( $\sigma/\mu$ ) of the gate delay increase with decreasing temperature [3]. Therefore, the worst-case  $\mu$  as well as the largest  $\sigma/\mu$  is observed at low temperatures (e.g., –40 °C), a variability analysis at the worst-case temperature is required. Therefore, in this paper, the temperature dependence of 256 within-die random gate delay variations ( $\sigma/\mu$ ) in sub-threshold logic circuits is measured in 40-nm CMOS test chips and is explained with a newly developed model. It is found that  $\sigma/\mu$  in sub-threshold logic circuits is proportional to  $1/T$  for the first time, where  $T$  is the absolute temperature.

This paper is organized as follows. Section II describes silicon measurements of the within-die distribution of the oscillation periods of ring oscillators (ROs) and the calculation of random component of the gate delay variations. In order

Manuscript received July 17, 2012; revised September 18, 2012; accepted October 29, 2012. Date of publication December 24, 2012; date of current version February 1, 2013. This brief was recommended by Associate Editor M. Alioto.

R. Takahashi, T. Yasufuku, H. Fuketa, and T. Sakurai are with the Institute of Industrial Science, University of Tokyo, Tokyo 153-8505, Japan (e-mail: ryo-taka@iis.u-tokyo.ac.jp).

H. Takata, M. Nomura, and H. Shinohara are with Semiconductor Technology Academic Research Center (STARC), Yokohama 222-0033, Japan.

M. Takamiya is with the VLSI Design and Education Center (VDEC), University of Tokyo, Tokyo 153-8505, Japan.

Digital Object Identifier 10.1109/TCSII.2012.2231038

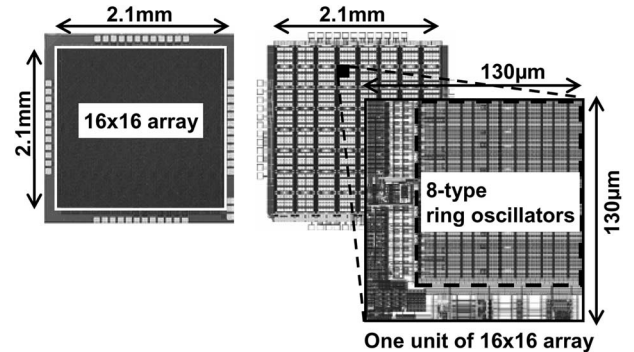


Fig. 1. Chip micrograph and layout of the device matrix array (DMA) test chip in 40-nm CMOS.

to investigate the dependence of the gate delay variation on temperature at low  $V_{DD}$ , a new model of the temperature dependence of the gate delay variations is proposed in Section III. Finally, Section IV concludes this paper.

## II. MEASUREMENT OF WITHIN-DIE RANDOM GATE DELAY VARIATIONS

### A. Test Chip Design

In order to measure the within-die random variation of the gate delay dependence on the supply voltage and the temperature efficiently, a device matrix array (DMA) test chip is designed and fabricated in 40-nm low-V<sub>th</sub> (LVT) CMOS technology.

Fig. 1 shows the chip micrograph and layout. The device under testing is a  $16 \times 16$  array with a 2.1-mm square. Each unit with a 130-μm square includes eight-type ROs.

Fig. 2 shows a schematic of the DMA. The oscillation periods of ROs are measured and the variability among 256 ROs is analyzed. The ROs are in the variable supply voltage region and the output of ROs are level-shifted to the nominal voltage (= 1.1 V). The measured eight-type ROs and measurement conditions are shown in Table I and Table II. The 11-stage ROs at 0.7 V and 1.1 V, and 31-stage ROs at 1.1 V, are not measured, since the oscillation frequencies are too fast to be measured in our measurement setup. Two-input NAND gate with  $\times 2$  drivability and two-input NOR gate with  $\times 2$  drivability are used. These ROs are designed so that the every gate has the same fan-out.

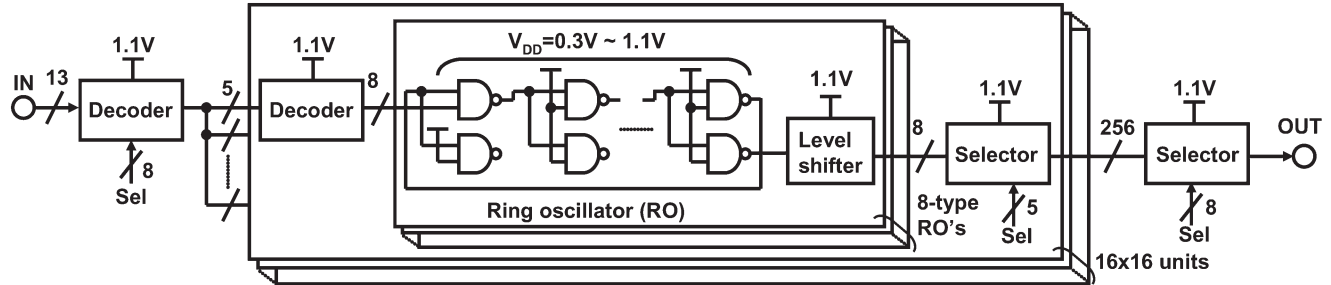


Fig. 2. Schematic of the DMA. The measurement circuit consists of  $16 \times 16 \times 8 (= 2048)$  ROs.

TABLE I  
TYPES OF RING OSCILLATORS UNDER TEST

NAND	11-stage	NOR	11-stage
	31-stage		31-stage
	85-stage		85-stage
	241-stage		241-stage

TABLE II  
MEASUREMENT CONDITIONS

Supply voltage [V]	0.3 / 0.5 / 0.7 / 1.1
Temperature [°C]	-40 / -20 / 0 / 25 / 50 / 85

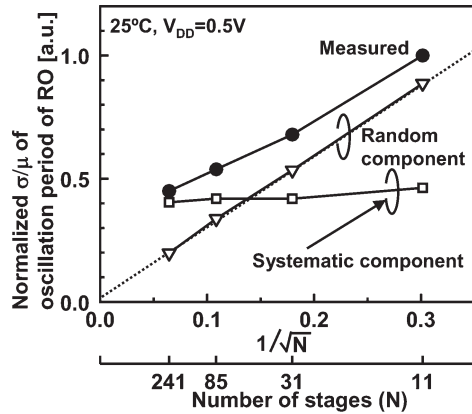


Fig. 3. Measured dependence of the normalized  $\sigma/\mu$  of the oscillation period on the number of stages ( $N$ ) of RO at  $V_{DD} = 0.5$  V and  $25$  °C. Random component of variation of NAND RO cycle time is inversely proportional to the square of number of stages.

### B. Measurement Results

Fig. 3 shows the measured dependence of the normalized  $\sigma/\mu$  of the oscillation period on the number of stages ( $N$ ) at  $V_{DD} = 0.5$  V and  $25$  °C.  $\sigma/\mu$  is normalized to the 11-stage RO. In order to separate the random variability component and the systematic variability component from the measured raw data, the fourth-order polynomial fitting proposed in [4] is used in this paper. The extracted random component is inversely proportional to the square root of  $N$ , which confirms the validity of the separation.

Figs. 4 and 5 show the measured temperature dependence of normalized mean ( $\mu$ ) and variation ( $\sigma/\mu$ ) of NAND and NOR gate delay with different  $V_{DD}$ , respectively. In Figs. 4 and 5,  $\mu$  and  $\sigma/\mu$  are normalized to the NAND gate at  $1.1$  V and  $25$  °C. In Fig. 4, the worst-case (= largest)  $\mu$  is observed at  $0.3$  V and  $-40$  °C, where the normalized  $\mu$  is more than  $10^4$ . In Fig. 5, the worst-case (= largest)  $\sigma/\mu$  is also observed at

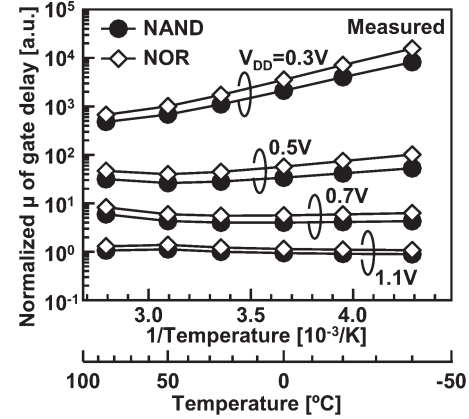


Fig. 4. Measured temperature dependence of normalized mean ( $\mu$ ) of NAND and NOR gate delay in 85-stage ROs with different  $V_{DD}$ .

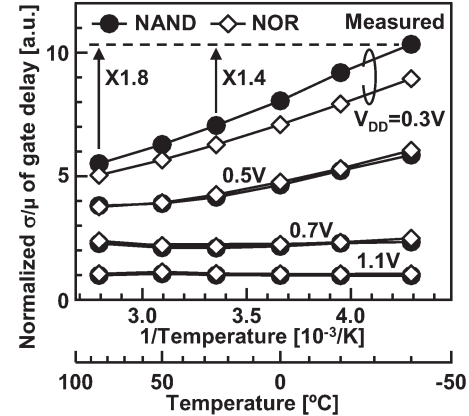


Fig. 5. Measured temperature dependence of normalized variation ( $\sigma/\mu$ ) of NAND and NOR gate delay in 85-stage ROs with different  $V_{DD}$ .

$0.3$  V and  $-40$  °C, where the normalized  $\sigma/\mu$  is more than  $10$ . In the NAND gate at  $0.3$  V,  $\sigma/\mu$  at  $-40$  °C is  $1.4$  times of that at  $25$  °C, and  $1.8$  times of that at  $85$  °C. The temperature dependence of  $\sigma/\mu$  in the sub-threshold logic circuits is not negligible. Therefore, the temperature dependence of  $\sigma/\mu$  is modeled in the next section.

### III. MODELING OF TEMPERATURE DEPENDENCE OF GATE DELAY VARIATIONS

#### A. Temperature Dependence of Gate Delay Variations in the Above-Threshold Region

In this section,  $\sigma/\mu$  of the gate delay in the above-threshold region is modeled. In the above-threshold region, on current

$(I_{ON})$  is modeled by the alpha-power law MOSFET model [5] as

$$I_{ON} = I_O(V_{DD} - V_{TH})^\alpha \quad (1)$$

where  $\alpha$  is the velocity saturation index and  $I_O$  is a technology-dependent parameter. Let  $t_{pd}$  be a gate delay and it is given by

$$t_{pd} = b \frac{CV_{DD}}{I_{ON}} = \frac{bCV_{DD}}{I_O(V_{DD} - V_{TH})^\alpha} \quad (2)$$

where  $b$  is a proportional constant and  $C$  is the load capacitance. The gate delay variation ( $\Delta t_{pd}$ ) induced by the  $V_{TH}$  variation ( $\Delta V_{TH}$ ) can be expressed by the first-order approximation as

$$\begin{aligned} \Delta t_{pd} &= \frac{dt_{pd}}{dV_{TH}} \Delta V_{TH} = \frac{b\alpha CV_{DD}}{I_O(V_{DD} - V_{TH})^{\alpha+1}} \Delta V_{TH} \\ &= t_{pd} \frac{\alpha}{V_{DD} - V_{TH}} \Delta V_{TH}. \end{aligned} \quad (3)$$

When  $\Delta V_{TH}$  is  $\sigma_{VTH}$ , which is defined as the standard deviation of the within-die  $V_{TH}$  variation,  $\Delta t_{pd}$  corresponds to the standard deviation of the gate delay variation ( $\sigma$ ). Therefore,  $\sigma/\mu$  of the gate delay due to the within-die random  $V_{TH}$  variation is derived from (3) as

$$\frac{\sigma}{\mu} = \frac{\Delta t_{pd}}{t_{pd}} = \frac{\alpha}{V_{DD} - V_{TH}} \Delta V_{TH} = \frac{\alpha}{V_{DD} - V_{TH}} \sigma_{VTH}. \quad (4)$$

In this paper, we assume that  $\alpha$  and  $\sigma_{VTH}$  do not depend on temperature for simplicity, since the dependence of  $\sigma_{VTH}$  on temperature is small, as reported in [6]. The dependence of  $\sigma/\mu$  of the gate delay on temperature is derived as

$$\frac{d\left(\frac{\sigma}{\mu}\right)}{dT} = \frac{\alpha\kappa\sigma_{VTH}}{(V_{DD} - V_{TH})^2} \quad (5)$$

where  $\kappa$  is the temperature coefficient for  $V_{TH}$  and given by

$$V_{TH}(T) = V_{TH}(T_0) - \kappa(T - T_0) \quad (6)$$

where  $V_{TH}(T)$  is  $V_{TH}$  at the temperature of  $T$  and  $T_0$  is the nominal temperature. At the nominal supply voltage of 1.1 V,  $(V_{DD} - V_{TH})^2$  is much larger than  $\alpha\kappa\sigma_{VTH}$  and, hence, the dependence of  $\sigma/\mu$  of the gate delay on temperature is significantly small, as shown in Fig. 5.

### B. Temperature Dependence of Gate Delay Variations in the Sub-Threshold Region

In this section,  $\sigma/\mu$  of the gate delay in the sub-threshold region is modeled. In the sub-threshold region,  $I_{ON}$  is expressed as

$$I_{ON} = I_O \exp\left(\frac{q}{nkT}(V_{DD} - V_{TH})\right) \cdot \left(1 - \exp\left(-\frac{qV_{DD}}{kT}\right)\right) \quad (7)$$

where  $n$  is the sub-threshold swing parameter,  $k$  is the Boltzmann constant,  $q$  is the elementary charge,  $T$  is the absolute temperature, and  $I_0$  is a technology-dependent parameter [7]. When  $V_{DD}$  is more than 0.1 V,  $I_{ON}$  is approximated to

$$I_{ON} \cong I_O \exp\left(\frac{q}{nkT}(V_{DD} - V_{TH})\right). \quad (8)$$

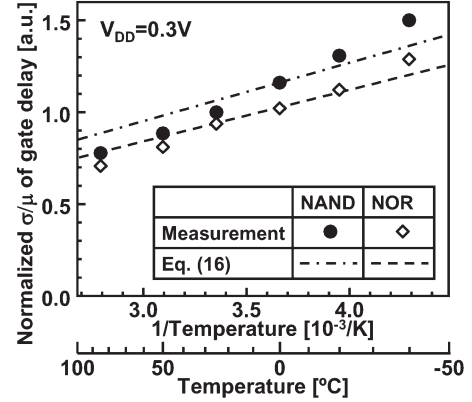


Fig. 6. Measured and calculated temperature dependence of normalized variation ( $\sigma/\mu$ ) of NAND and NOR gate delay in 85-stage ROs at 0.3 V.

Here,  $X_{VTH}$  is introduced to express the within-die random  $V_{TH}$  variation as

$$V_{TH} = V_{TH0} + X_{VTH}, \quad (9)$$

$$X_{VTH} \sim N(0, \sigma_{VTH}^2) \quad (10)$$

where  $\sigma_{VTH}$  is the standard deviation of the within-die random  $V_{TH}$  variation and  $V_{TH0}$  is the mean of the  $V_{TH}$  variation.

A gate delay ( $t_{pd}$ ) in the sub-threshold region is derived as

$$t_{pd} = d \frac{CV_{DD}}{I_{ON}} = A \exp\left(\frac{q}{nkT} X_{VTH}\right) \quad (11)$$

where  $d$  is a proportional constant and

$$A = \frac{dCV_{DD}}{I_O \exp\left(\frac{q}{nkT}(V_{DD} - V_{TH0})\right)}. \quad (12)$$

Equation (11) indicates that the variation of the gate delay in the sub-threshold region follows log-normal distribution. Therefore, the mean and the variance of the gate delay variation are given by

$$\mu = A \exp\left(\frac{\left(\frac{q\sigma_{VTH}}{nkT}\right)^2}{2}\right), \quad (13)$$

$$\sigma^2 = A^2 \exp\left(\left(\frac{q\sigma_{VTH}}{nkT}\right)^2\right) \left\{ \exp\left(\left(\frac{q\sigma_{VTH}}{nkT}\right)^2\right) - 1 \right\}. \quad (14)$$

Consequently,  $\sigma/\mu$  of the gate delay is derived as

$$\frac{\sigma}{\mu} = \sqrt{\exp\left(\left(\frac{q\sigma_{VTH}}{nkT}\right)^2\right) - 1}. \quad (15)$$

When  $(q\sigma_{VTH}/nkT)^2 \ll 1$ , (15) can be approximated to

$$\frac{\sigma}{\mu} \cong \sqrt{\left\{1 + \left(\frac{q\sigma_{VTH}}{nkT}\right)^2\right\} - 1} = \frac{q\sigma_{VTH}}{nkT}. \quad (16)$$

Since the dependence of  $\sigma_{VTH}$  on temperature is small [6], (16) shows that  $\sigma/\mu$  in the sub-threshold region is proportional to  $1/T$ , which is clarified for the first time. Equation (16) is compared with the measured results in Fig. 6. It should be noted that  $\sigma_{VTH}$  in (16) is estimated by the least squares method. Fig. 6 shows the measured and calculated temperature

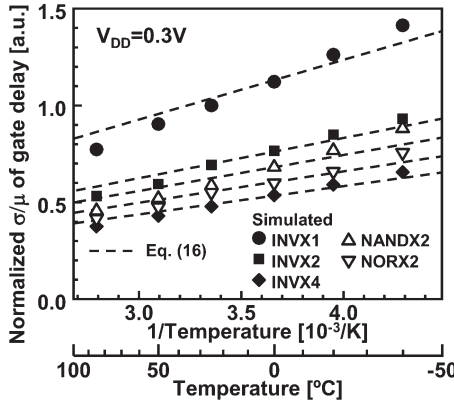


Fig. 7. SPICE simulated and calculated temperature dependence of normalized variation ( $\sigma/\mu$ ) of five-type gate delay in 11-stage ROs with different  $V_{DD}$ .

dependence of normalized  $\sigma/\mu$  of NAND and NOR gate delay at 0.3 V.  $\sigma/\mu$  is normalized to the NAND gate at 25 °C. Equation (16) is a good approximation to the measured temperature dependence of the gate delay variations, since the relative errors between the measured and calculated results are less than 11%.

In Fig. 6, only NAND and NOR gates are shown. In order to investigate the temperature dependence in various gates, five-type gates are simulated with SPICE and compared with the calculated results by (16). Fig. 7 shows the SPICE simulated and calculated temperature dependence of normalized  $\sigma/\mu$  of the five-type gates at 0.3 V. Three-type inverters with  $\times 1$  drivability,  $\times 2$  drivability, and  $\times 4$  drivability are added.  $\sigma/\mu$  is normalized to the inverter with  $\times 1$  drivability at 25 °C. The simulated results are obtained by 3000 times Monte-Carlo SPICE. Fig. 7 indicates that (16) is a good approximation to the simulated temperature dependence of the gate delay variations, since the relative errors between the simulated and calculated results are less than 12%. As the inverter drivability is reduced,  $\sigma/\mu$  increases, because the random  $V_{TH}$  variations increase with reducing transistor size.

#### IV. CONCLUSION

In this paper, the temperature dependence of the within-die random gate delay variations in sub-threshold logic circuits is measured in 40-nm CMOS test chips. When the temperature is reduced from 25 °C to -40 °C, the sigma/average ( $\sigma/\mu$ ) of the gate delay at 0.3 V increases by 1.4 times. A newly developed model shows that variation ( $\sigma/\mu$ ) of the gate delay is proportional to  $1/T$  for the first time, where  $T$  is the absolute temperature. Therefore, the large delay variations at low temperatures should be considered in the worst-case design of the sub-threshold logic circuits.

#### ACKNOWLEDGMENT

This work was carried out as a part of the Extremely Low Power project supported by the Ministry of Economy, Trade, and Industry and the New Energy and Industrial Technology Development Organization.

#### REFERENCES

- [1] A. Wang, B. Calhoun, and A. Chandrakasan, *Sub-Threshold Design for Ultra Low-Power Systems*. New York: Springer-Verlag, 2006.
- [2] N. Drego, A. Chandrakasan, and D. Boning, "All-digital circuits for measurement of spatial variation in digital circuits," *IEEE J. Solid-State Circuits*, vol. 45, no. 3, pp. 640–651, Mar. 2010.
- [3] D. Bol, C. Hocquet, D. Flandre, and J.-D. Legat, "The detrimental impact of negative celsius temperature on ultra-low-voltage CMOS logic," in *Proc. ESSCIRC*, Sep. 2010, pp. 522–525.
- [4] H. Masuda, S. Ohkawa, A. Kurokawa, and M. Aoki, "Challenge: Variability characterization and modeling for 65- to 90-nm processes," in *Proc. IEEE CICC*, Sep. 2005, pp. 593–599.
- [5] T. Sakurai and A. Newton, "Alpha-power law MOSFET model and its applications to CMOS inverter delay and other formulas," *IEEE J. Solid-State Circuits*, vol. 25, no. 2, pp. 584–594, Apr. 1990.
- [6] T. Tsunomura, A. Nishida, and T. Hiramoto, "Investigation of threshold voltage variability at high temperature using Takeuchi plot," *Jpn. J. Appl. Phys.*, vol. 49, no. 5, pp. 054101-1–054101-6, May 2010.
- [7] H. Fuketa, S. Iida, T. Yasufuku, M. Takamiya, M. Nomura, H. Shinohara, and T. Sakurai, "A closed-form expression for estimating minimum operating voltage ( $V_{DDmin}$ ) of CMOS logic gates," in *Proc. ACM/EDAC/IEEE Des. Autom. Conf.*, Jun. 2011, pp. 984–989.